Optical and Quantum Electronics (2020) 52:430
https://doi.org/10.1007/s11082-020-02547-7

Performance assessment of hybrid PPM–BPSK–SIM based FSO communication system using time and wavelength diversity under variant atmospheric turbulence

Kanchan Sharma[1] · **Surender K. Grewal**[1]

Received: 19 January 2019 / Accepted: 11 September 2020 / Published online: 21 September 2020

Abstract
In this paper, free space optical communication system employing a hybrid modulation technique called pulse position modulation–binary phase shift keying–subcarrier intensity modulation technique, is investigated using wavelength and time diversity, by considering log-normal and gamma–gamma probability density function as the channel-fading statistics under weak, moderate and strong turbulence. The analytical average bit error rate and closed form of expression of the proposed hybrid modulation scheme are derived. The outcomes of the simulation demonstrate the outstanding consistency of the derived closed form expression with those achieved by the Gauss–Hermite approximation and the Monte Carlo simulations.

Keywords Atmospheric turbulence · Bit error rate · Free space optical communication system · Signal to noise ratio · Subcarrier intensity modulation · Time diversity · Wavelength diversity

1 Introduction

Free space optical communication system (FSO) is license free and is one of the most promising wireless communication technique which enables to offer extremely large capacity, high-immunity to interference, low-latency, low-energy consumption, high data rate of transmission, reliable and secure communications. Consequently, FSO expresses intensive demand in indoor and outdoor communication system as an alternative to radio frequency communication. Inspite of number of advantages for employing FSO, the efficiency of communication of the FSO systems is reduced in adverse atmospheric conditions. As a consequence, the FSO system is degraded by atmospheric turbulence (AT) which causes fading and misalignment losses. The adverse effect of intensity fluctuation or fading during propagation is attributable to the phenomenon of inhomogeneity of pressure and temperature in the optical transmission path. The optical channel displays predictably time-variant

✉ Kanchan Sharma
joinkanchansharma@gmail.com

1 DCRUST, Murthal, Sonepat, India

characteristics modeled to measure the consistency of the communication channel. A variety of statistical models to explain AT have been presented in the literature. The numerous models represent amplitude variations with respect to turbulence magnitude strengths that are negative exponential, gamma–gamma, I–K distribution and lognormal, etc. Weak AT is modeled as a lognormal distribution, whereas moderate and strong AT is modeled as a gamma–gamma (GG) distribution.

In literature researchers investigated intensity-modulation/direct-detection based On–Off keying (OOK) modulation scheme which is most widely accepted scheme due to its easy implementation and less cost (Zhu and Kahn 2002). But it is noted that OOK based FSO systems experiences unacceptable performance over atmospheric turbulence channels (Majumdar 2014). Then, the power efficient pulse position modulation (PPM) has been considered to be used in FSO communication systems. However, PPM required symbol synchronization and have poor bandwidth efficiency (Viswanath et al. 2016). Another a competitive alternative for the OOK is the Subcarrier Intensity Modulation (SIM) (Li et al. 2007). The performance of Binary Phase Shift Keying (BPSK) SIM in FSO systems was then extensively investigated (Popoola and Ghassemlooy 2009). The performance of BPSK–SIM in terms of average bit error rate (BER) is investigated and observed that it experiences better performance in comparison with the other coherent and non coherent modulation schemes (Popoola and Ghassemlooy 2009). However, the power efficiency of BPSK–SIM is poor in comparison to PPM technique (Ghassemlooy et al. 2012). Thus, by integrating PPM and BPSK–SIM modulation schemes, hybrid modulation scheme based FSO system has been presented which overcomes these limitations and also results better BER performance (Faridzadeh et al. 2012; Liu et al. 2015; Giri and Patnaik 2018)

Since average BER is a vital quantitative performance metric that represents the robustness of the received signal over wireless path. The average BER of a hybrid modulated FSO system can be mathematically expressed as the expectation of conditional BER over the probability density function (pdf) of AT fading. The average BER expression of FSO systems employing hybrid modulation schemes involve integrals of Gaussian Q-function along with lognormal pdf (Faridzadeh et al. 2012; Liu et al. 2015; Giri and Patnaik 2018). Therefore, the accurate computation of closed form expression having such integrals is mathematically unsolvable and makes it difficult to properly analyze the average BER performance of the system. Alternatively, closed form expression is rigorously evaluated for the average BER of hybrid modulated FSO systems with weak, moderate and strong AT using numerical methods like exponential approximation of Gaussian Q-function (Chiani et al. 2003). Olabiyi and Annamalai (2012) typically presented a exponential approximation of Gaussian Q-function. Khandelwal et al. (2014) presented an possible approximation of symbol error rate (SER) probability for radio frequency wireless communication systems over weak AT link. Héliot et al. (2008); Kaushik et al. (2018); Sharma and Grewal (2020) presented the probable derivation of approximate closed form expressions for BER and ergodic channel capacity of FSO communication system using different existing coherent and non-coherent digital modulation schemes over lognormal fading channel.

The proper implementation of an efficient modulation scheme, coding scheme, diversity, aperture averaging can mitigate these channel effects (Abaza et al. 2014; Gappmair and Flohberger 2009; Feng et al. 2014; Navidpour et al. 2007). The diversity is found to be an excellent solution to combat the degradation occurs in signal due to the active presence of AT. Diversity may be categorized as time diversity, wavelength diversity, polarisation diversity and spatial diversity. Time diversity conventionally uses a single transceiver pair, same bits of information transmitted in effective number of different time slots (Ji et al. 2020, 2019; Nistazakis 2013; Balaji and Prabu 2018). In wavelength diversity, composite transmitter transmits same bits of information over different wavelength simultaneously and are accurately detected by the respective wavelength receiver (Nouri and Uysal 2020; Shah and Kothari 2019; Srivastava et al. 2019; Wainright et al. 2005; Xarcha et al. 2012; Prabu et al. 2014). Polarisation diversity utilizes different polarisation modes for transmitting the bits of information (Zhang et al. 2019; Islam and Majumder 2020; Yang 2013; Trisno and Davis 2006). Spatial diversity traditionally employs multiple transmitters and multiple receivers for carrying out transmission of bits of information using same single wavelength (Khichar and Inaniya 2020; Ding et al. 2020; Tsiftsis et al. 2009; Varotsos et al. 2019).

To improve remarkably the average BER performance, a hybrid modulation scheme PPM–BPSK–SIM (pulse position modulation–binary phase shift keying–subcarrier intensity modulation) FSO communication system with time and wavelength diversity, is proposed in the paper. The results of the proposed system are analysed for variant AT conditions. The closed form expression for average BER is derived for both time and wavelength diversity which is more simpler and accurate in comparison to Gauss Hermite approximation and consistent with the Monte Carlo simulation. It is also analyzed for varying length of symbol and diversity parameters.

The paper is organized as follows, In Sect. 2, discusses system description, log-normal turbulence and GG turbulence channel model. Section 3 describes a hybrid PPM–BPSK–SIM based FSO communication system. In Sect. 4, a derivation of proposed approximate average BER closed form expression using no diversity, wavelength diversity and time diversity is presented for hybrid FSO systems under weak, moderate and strong AT condition. In Sect. 5 numerical results are analyzed and conclusions are set out in Sect. 6.

2 FSO system and turbulence channel model

In FSO communication over the atmospheric channel, the amplitude distortion and phase distortion of the modulated optical signal occurred due to signal absorption and dispersion in the prominent presence of haze, cloud, rain, fog, snow and dust in the atmospheric channel. Figure 1 shows the diagram of FSO communication system. The total channel attenuation which realistically is the direct sum of geometric loss and atmospheric attenuation and is given as

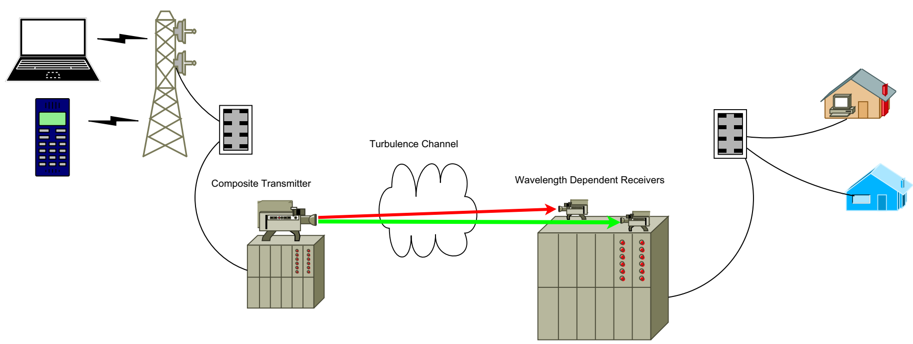

Fig. 1 FSO communication system

$$\alpha_r = \frac{A_e}{\pi\left(\frac{\phi_r L_d}{2}\right)^2} \cdot \exp\left(-\eta L_d\right) \tag{1}$$

where A_e, ϕ_r, η, L_d is the the receiver's aperture area, the angle of divergence, the atmospheric extinction coefficient and the link distance respectively. The proposed research assumes without loss of generality the turbulent distribution of the FSO channel model as a lognormal distribution over weak AT condition and gamma–gamma (GG) distribution under moderate and strong AT situation. In a weak turbulent FSO communication system, the lognormal probability density function (pdf) of the laser intensity is given as (Shankar 2017)

$$p(I_m) = \frac{1}{I_m \sigma_{R_m} \sqrt{2\pi}} \cdot \exp\left(- \frac{\left(\ln\left(\frac{I_m}{I_{m_o}}\right) + \frac{\sigma^2_{R_m}}{2} \right)^2}{2\sigma^2_{R_m}} \right), \quad I_m \geq 0 \tag{2}$$

where the average laser irradiance received in presence of no AT is I_{m_o}. The parameter $\sigma^2_{R_m}$ is the variance in the log intensity of the optical turbulence termed as the Rytov variance, defined as

$$\sigma^2_{R_m} = 1.23 k^{7/6} L_d^{11/6} C_n^2 \tag{3}$$

where k is the wave number and its value is equal to $2\pi/\lambda$, L_d is the optical transmission link distance between transmitter and receiver and C_n^2 is the refractive index structure parameter that remains unchanged for the complete duration of optical transmission. Particularly, $\sigma^2_{R_m} \leq 1$ in case of weak AT.

An FSO link that experiences moderate and strong AT for which GG pdf of the laser intensity is given by (Shankar 2017)

$$p_{I_m}(I_m) = \frac{2(\alpha_m \beta_m)^{\frac{\alpha_m+\beta_m}{2}}}{\Gamma(\alpha_m)\Gamma(\beta_m)} I_m^{\frac{\alpha_m+\beta_m-2}{2}} K_{\alpha_m-\beta_m}\left(2\sqrt{\alpha_m \beta_m I_m}\right), \quad I_m > 0 \tag{4}$$

where K_v is the modified Bessel function of second kind of v order, $\Gamma(\cdot)$ is the gamma function, α_m and β_m is the associated channel parameter which can be expressed as (Uysal et al. 2006)

$$\alpha_m = \left[\exp\left(0.49\sigma^2_{R_m}\left(1 + 0.56\sigma^{12/5}_{R_m}\right)^{-7/6}\right) - 1\right]^{-1} \tag{5a}$$

$$\beta_m = \left[\exp\left(0.51\sigma^2_{R_m}\left(1 + 0.69\sigma^{12/5}_{R_m}\right)^{-5/6}\right) - 1\right]^{-1} \tag{5b}$$

In the proposed hybrid modulation scheme under weak AT condition, assumption is made that the sum of N lognormal random variable is considered for computation and is $\zeta_m = \frac{I_{m_1}+I_{m_2}+I_{m_3}+\cdots+I_{m_N}}{I_{m_o}} = \exp(V_m)$. The probability density function is given as (Liu et al. 2015)

$$p(\zeta_m) = \frac{1}{\zeta_m \sigma_{\zeta_m} \sqrt{2\pi}} \cdot \exp\left(-\frac{(\ln(\zeta_m) - V_{\zeta_m})^2}{2\sigma^2_{\zeta_m}}\right) \tag{6}$$

where the resultant mean is $V_{\zeta_m} = \ln(N) - \frac{1}{2}\ln\left[1 + \frac{\exp(\sigma^2_{R_m})-1}{N}\right]$ and variance is $\sigma^2_{\zeta_m} = \ln\left[1 + \frac{\exp(\sigma^2_{R_m})-1}{N}\right]$. In case of moderate and strong AT condition, assumption is made that the sum of N gamma–gamma random variable is considered for computation and can be approximated as single GG distribution (Chatzidiamantis and Karagiannidis 2011).

3 FSO communication system using PPM-BPSK-SIM

In hybrid FSO communication system, a block containing $N = \log_2 K$ data bits is transformed into PPM symbol formats (N is number of bits per symbol, and K is the average length of the symbol) which is carefully followed by the parallel to serial conversion that results into a new stream of data. The resulted stream of generated data is modulated into the subcarrier signal using BPSK. A proper DC bias is instantly added to the modulated subcarrier to ensure it has non-negative values fed to the laser diode driving circuitry. The block diagram of the transmitter and receiver of hybrid PPM–BPSK–SIM FSO is shown in Fig. 2. The transmitted optical signal of proposed hybrid FSO system is given as

$$x(t) = \sum_{m=1}^{N} I_m\left[1 + \mu_o cos(2\pi f_c t + b_m \pi) p(t - (m-1)T_s)\right] \tag{7}$$

where I_m denotes the corresponding transmitter intensity of m th code generated, μ_o represent the modulation index, T_s is the one code element duration, p(t) represent rectangular pulse with a duration of one time slot and f_c represents the carrier frequency.

On the receiving end, the optical signal received from the atmospheric channel is extracted by the optical bandpass filter and translated back to the electrical signal by the optical receiver. The regenerated photocurrent varies in accordance with the observed variation in the instantaneous modulated signal and is adequately defined for one symbol duration as

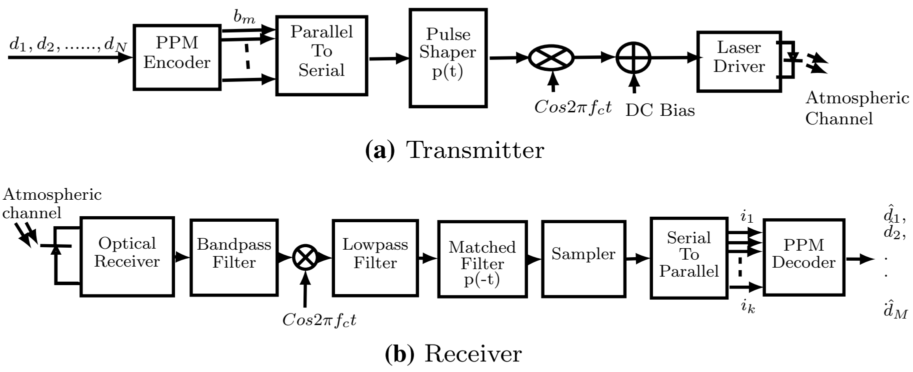

Fig. 2 Hybrid PPM–BPSK–SIM FSO communication system with no diversity

$$i(t) = RG_r\alpha_r \sum_{m=1}^{N} I_m\left[1 + \mu_o cos(2\pi f_c t + b_m\pi)p(t-(m-1)T_s)\right] + n_r(t) \tag{8}$$

where R is the responsivity of optical receiver, G_r is the optical receiver gain, α_r is the channel attenuation and $n_r(t)$ is the sum of thermal noise and receiver shot noise. The variance of optical receiver noise can be described as

$$\sigma^2_{n_r} = \sigma^2_{t,n} + \sigma^2_{s,n} = \frac{4K_bTF_n}{R_{Load}}\frac{R_b}{2} + 2qR\alpha_r G_r^2 I\frac{R_b}{2}\left[K_aG_r + (1-K_a)\left(2-\frac{1}{G_r}\right)\right] \tag{9}$$

where K_b is the Boltzmann constant, q is the charge of electron, T is the receiver ambient noise temperature, F_n is amplifier noise figure, K_a is the ionization factor and R_b is the bit rate of the system (Liu et al. 2015).

The output coherent receiver current i_{cd} for one symbol duration is given by

$$i_{cd}(t) = \frac{RG_r\alpha_r}{2}\sum_{m=1}^{N} I_m + n_{cd}(t) \tag{10}$$

where $n_{cd}(t)$ represents the Additive White Gaussian Noise (AWGN) whose variance is equal to $\frac{\sigma^2_{K-PPM}}{2}$ and $\sigma^2_{K-PPM} = \frac{\eta R_b K}{2N}$. The double sided power spectral density of the AWGN is equal to η (Faridzadeh et al. 2012; Liu et al. 2015; Giri and Patnaik 2018).

Finally, the demodulation is promptly done by properly obtaining the maximum absolute signal in one symbol duration and its precise position within symbol instantly decides the received data of N bits.

4 BER analysis of proposed system

The average BER of hybrid PPM–BPSK–SIM based FSO communication system over weak, moderate and strong turbulence is properly investigated for no diversity, wavelength diversity and time diversity.

4.1 BER analysis under weak AT

The weak AT channel is mathematically modelled as lognormal distribution as described in the Eq. 6. The average BER of hybrid modulation scheme based FSO communication system with no diversity, wavelength diversity and tine diversity is presented below.

4.1.1 No diversity

In the case of no diversity scheme, only one pair of transceivers is used. The instantaneous conditional BER of hybrid PPM–BPSK–SIM modulation scheme employed in FSO communication system is expressed as

$$P_{ec}(\zeta) = Q\left(\sqrt{\gamma_i}\right) = Q\left(\sqrt{\bar{\gamma} I_o^2 \zeta^2}\right) \tag{11}$$

where γ_i is the instantaneous SNR, $\bar{\gamma}$ is the average electrical SNR and its expression for the hybrid scheme as given by

$$\bar{\gamma} = \left(\frac{\mu_o R \alpha_r}{2\sigma_{K-PPM}} \right)^2 \tag{12}$$

where Q(·) is the Gaussian-Q function.

The statistical expectation of instantaneous conditional BER obtained in Eq. 2 over the statistical lognormal fading random variable ζ and the appropriate expression of unconditional BER or average BER is given as

$$P_e = E[P_{ec}] = \int_0^\infty P_{ec}(\zeta) p(\zeta) d\zeta \tag{13}$$

where p(ζ) is the pdf of lognormal turbulence channel model given in Eq. 6. The closed approximation limit of Gaussian-Q function is expressed in terms of weighted sum of exponential form (Olabiyi and Annamalai 2012). The Gaussian-Q function is approximated upto second order which is given as

$$Q(\sqrt{I}) \approx \frac{u_0}{2} e^{-\frac{vI}{2}} + \frac{u_1}{2} e^{-vI} \tag{14}$$

where $u_0 = 0.3070$, $u_1 = 0.4389$ and v = 1.0520.

Using Eqs. 2, 14 and 6 in Eq. 13, the Average BER or unconditional BER can be re-expressed as

$$\begin{aligned} P_e &= \int_0^\infty \left(\frac{u_0}{2} e^{-\frac{v\bar{\gamma} I_o^2 \zeta^2}{2}} + \frac{u_1}{2} e^{-v\bar{\gamma} I_o^2 \zeta^2} \right) \cdot \frac{1}{\zeta \sigma_\zeta \sqrt{2\pi}} \cdot \exp\left(-\frac{\left(\ln(\zeta) - V_\zeta\right)^2}{2\sigma_\zeta^2} \right) d\zeta \\ &= \int_0^\infty \phi(\zeta) \cdot \frac{1}{\zeta \sigma_\zeta \sqrt{2\pi}} \cdot \exp\left(-\frac{\left(\ln(\zeta) - V_\zeta\right)^2}{2\sigma_\zeta^2} \right) d\zeta \end{aligned} \tag{15}$$

The lognormal integral mentioned in the Eq. 15 can be evaluated using the method presented by Wilck (2001). By employing, the Taylor series expansion of second order of the function of ln($\phi(\zeta)$) in term of ln(ζ) around the point ln(ζ_o), function ln($\phi(\zeta)$) can be expressed as

$$\ln(\phi(\zeta)) = \ln\left[\phi(\zeta_o) \cdot \left(\frac{\zeta}{\zeta_o} \right)^{\omega'} \cdot \exp\left(\frac{(\ln(\zeta) - \ln(\zeta_o))^2}{2} \omega'' \right) \right] \tag{16}$$

Thus, after taking antilogarithm on both sides we can say that

$$\phi(\zeta) = \phi(\zeta_o) \cdot \left(\frac{\zeta}{\zeta_o} \right)^{\omega'} \cdot \exp\left(\frac{(\ln(\zeta) - \ln(\zeta_o))^2}{2} \omega'' \right) \tag{17}$$

where, $\omega' = \left.\frac{\partial[\ln(\phi(\zeta))]}{\partial(\ln \zeta)}\right|_{\ln \zeta_o}$ and $\omega'' = \left.\frac{\partial^2[\ln(\phi(\zeta))]}{\partial(\ln \zeta)^2}\right|_{\ln \zeta_o}$

After substituting the value of $\phi(\zeta)$ in Eq. 15 obtained from Eq. 17, average BER of proposed system can be expressed as

$$P_e = \int_0^{\infty} \phi(\zeta_o) \cdot \left(\frac{\zeta}{\zeta_o}\right)^{\omega'} \cdot \exp\left(\frac{(\ln(\zeta) - \ln(\zeta_o))^2}{2}\omega''\right) \cdot \frac{1}{\zeta \sigma_\zeta \sqrt{2\pi}} \cdot \exp\left(-\frac{\left(\ln(\zeta) - V_\zeta\right)^2}{2\sigma_\zeta^2}\right) d\zeta \tag{18}$$

Lognormal distribution reduces to normal distribution by substituting $\psi = \ln(\zeta)$ in the integral Eq. 18

$$P_e = \int_{-\infty}^{\infty} \phi(\zeta_o) \cdot \left(\frac{e^{\psi}}{\zeta_o}\right)^{\omega'} \cdot \exp\left(\frac{(\psi - \psi_o)^2}{2}\omega''\right) \cdot \frac{1}{\sigma_\zeta \sqrt{2\pi}} \cdot \exp\left(-\frac{\left(\psi - V_\zeta\right)^2}{2\sigma_\zeta^2}\right) d\psi \tag{19}$$

After mathematical manipulations, Integral mentioned in Eq. 19 can be expressed as

$$\begin{aligned} P_e = {} & \frac{\phi(\zeta_o)}{\sigma_\zeta \sqrt{2\pi} (\zeta_o)^{\omega'}} \cdot \exp\left[\frac{(\sigma_\zeta^2 \omega' - \sigma_\zeta^2 \omega'' \psi_o + V_\zeta)^2}{2\sigma_\zeta^2 (1 - \sigma_\zeta^2 \omega'')} + \frac{(\sigma_\zeta^2 \omega'' \psi_o^2 - V_\zeta)^2)}{2\sigma_\zeta^2}\right] \\ & \cdot \int_{-\infty}^{\infty} \exp\left[-\left(\frac{1 - \sigma_\zeta^2 \omega''}{2\sigma_\zeta^2}\right)\left(\psi - \frac{\sigma_\zeta^2 \omega' - \sigma_\zeta^2 \omega'' \psi_o + V_\zeta}{1 - \sigma_\zeta^2 \omega''}\right)^2\right] d\psi \end{aligned} \tag{20}$$

Expression (20) can be solved mathematically and tractable simplified expressed of average BER or unconditional BER is given as

$$P_e = \frac{\phi(e^{\psi_o})}{\sqrt{1 - \sigma_\zeta^2 \omega''}} \cdot \left(\frac{e^{V_\zeta}}{e^{\psi_o}}\right)^{\omega'} \cdot \exp\left[\frac{(\omega' \sigma_\zeta)^2}{2} + \frac{\omega''(V_\zeta + \omega' \sigma_\zeta^2 - \psi_o)^2}{2(1 - \sigma_\zeta^2 \omega'')}\right] \tag{21}$$

Average BER expression mentioned in Eq. 21 attains the finite value if and only if the condition $\sigma_\zeta^2 \omega'' \le 1$ satisfies. The accuracy of the obtained average BER expression depend on the accurate selection of the reference point ψ_o which must be lies in the integrand obtained in Eq. 21 and obtained by V_ζ. Thus, necessary and sufficient condition resulted is given as

$$\psi_o = V_\zeta + \omega'(\psi_o)\sigma_\zeta^2 \tag{22}$$

Equation 22 can be solved using MATLAB software in order to obtain the value of ψ_o. Initially value of ψ_o is chosen to be equal to V_ζ. The closed form expression for average BER or unconditional BER for proposed hybrid PPM–BPSK–SIM FSO given in Eq. 21 can be evaluated using Eq. 22, ω' and ω''. After performing the simplification, the values of ω' and ω'' for hybrid FSO system are as follows

$$\omega'(\psi_o) = -\bar{\gamma} v I_o e^{2\psi_o} \cdot \left[1 + \frac{u_1}{u_1 + u_0 e^{\frac{\bar{\gamma} v I_o e^{2\psi_o}}{2}}}\right] \tag{23a}$$

$$\omega''(\psi_o) = 2\omega'(\psi_o) + \frac{u_0}{u_1} e^{\frac{\bar{\gamma} v I_o}{2} e^{2\psi_o}} \left[\omega' + \bar{\gamma} v I_o e^{2\psi_o}\right]^2 \tag{23b}$$

4.1.2 Wavelength Diversity

In the wavelength diversity scheme, Ξ_N different transceivers, Each of them instantly conveys the same signal using different wavelengths at the same time. Each *m th* copy of desired signal is captured by the assigned *m th* receiver. Thus, assuming independent and identically distributed (i.i.d) bit transmission, the conditional BER (P_{ec}) for multiple AT channels $m = 1, 2, \dots, \Xi_N$ is given by

$$P_{ec}(\zeta_m) = Q\left(\sqrt{\frac{\bar{\gamma}}{\Xi_N}\sum_{m=1}^{\Xi_N}\left(I_{m_0}\zeta_m\right)^2}\right) \tag{24}$$

The average BER for each wavelength link present in the wavelength diversity scheme is obtained by computing the expectation of unconditional BER over pdf of ζ_m, is given by

$$P_e = \int_0^\infty P_{ec}(\zeta_m)p_{\zeta_m}(\zeta_m)\mathrm{d}\zeta_m \tag{25}$$

By using Eq. 6 and Eq. 24 in Eq. 25, the unconditional BER is given as

$$P_e = \int_0^\infty Q\left(\sqrt{\frac{\bar{\gamma}}{\Xi_N}\sum_{m=1}^{\Xi_N}\left(I_{m_0}\zeta_m\right)^2}\right)\frac{1}{\zeta_m\sigma_{\zeta_m}\sqrt{2\pi}}\cdot\exp\left(-\frac{(\ln(\zeta_m)-V_{\zeta_m})^2}{2\sigma_{\zeta_m}^2}\right)\mathrm{d}\zeta_m \tag{26}$$

By substituting the value of Q function from Eq. 3 in Eq. 26, the simplified expression is given by

$$\begin{aligned} P_e = {} & \frac{u_0}{2}\prod_{m=1}^{\Xi_N}\int_0^\infty e^{\frac{-v\bar{\gamma}I_{m_O}^2\zeta_m^2}{2\Xi_N}}\frac{1}{\zeta_m\sigma_{\zeta_m}\sqrt{2\pi}}\cdot\exp\left(-\frac{(\ln(\zeta_m)-V_{\zeta_m})^2}{2\sigma_{\zeta_m}^2}\right)\mathrm{d}\zeta_m \\ & + \frac{u_1}{2}\prod_{m=1}^{\Xi_N}\int_0^\infty e^{\frac{-v\bar{\gamma}I_{m_O}^2\zeta_m^2}{\Xi_N}}\frac{1}{\zeta_m\sigma_{\zeta_m}\sqrt{2\pi}}\cdot\exp\left(-\frac{(\ln(\zeta_m)-V_{\zeta_m})^2}{2\sigma_{\zeta_m}^2}\right)\mathrm{d}\zeta_m \end{aligned} \tag{27}$$

Assuming $\phi^{(1)}(I_m) = e^{\frac{-v\bar{\gamma}I_{m_O}^2\zeta_m^2}{2\Xi_N}}$ and $\phi^{(2)}(\zeta_m) = e^{\frac{-v\bar{\gamma}I_{m_O}^2\zeta_m^2}{\Xi_N}}$ and the Eq. 27 can be rewrite as

$$\begin{aligned} P_e = {} & \frac{u_0}{2}\prod_{m=1}^{\Xi_N}\int_0^\infty \phi^{(1)}(\zeta_m)\frac{1}{\zeta_m\sigma_{\zeta_m}\sqrt{2\pi}}\cdot\exp\left(-\frac{(\ln(\zeta_m)-V_{\zeta_m})^2}{2\sigma_{\zeta_m}^2}\right)\mathrm{d}\zeta_m \\ & + \frac{u_1}{2}\prod_{m=1}^{\Xi_N}\int_0^\infty \phi^{(2)}(\zeta_m)\frac{1}{\zeta_m\sigma_{\zeta_m}\sqrt{2\pi}}\cdot\exp\left(-\frac{(\ln(\zeta_m)-V_{\zeta_m})^2}{2\sigma_{\zeta_m}^2}\right)\mathrm{d}\zeta_m \end{aligned} \tag{28}$$

Using Eqs. 15, 17, 18 and 21 in Eq. 28, the BER expression can be written as

$$P_e = \frac{u_0}{2}\prod_{m=1}^{\Xi_N}\frac{\phi^{(1)}(e^{\psi_o^{(1)}})}{\sqrt{1-\sigma_{\zeta_m}^2\,\omega_1''}}\cdot\left(\frac{e^{V_{\zeta_m}}}{e^{\psi_o^{(1)}}}\right)^{\omega_1'}\cdot\exp\left[\frac{(\omega_1'\sigma_{\zeta_m})^2}{2}+\frac{\omega_1''(V_{\zeta_m}+\omega_1'\sigma_{\zeta_m}^2-\psi_o^{(1)})^2}{2(1-\sigma_{\zeta_m}^2\,\omega_1'')}\right]$$
$$+\frac{u_1}{2}\prod_{m=1}^{\Xi_N}\frac{\phi^{(2)}(e^{\psi_o^{(2)}})}{\sqrt{1-\sigma_{\zeta_m}^2\,\omega_2''}}\cdot\left(\frac{e^{V_{\zeta_m}}}{e^{\psi_o^{(2)}}}\right)^{\omega_2'}\cdot\exp\left[\frac{(\omega_2'\sigma_{\zeta_m})^2}{2}+\frac{\omega_2''(V_{\zeta_m}+\omega_2'\sigma_{\zeta_m}^2-\psi_o^{(2)})^2}{2(1-\sigma_{\zeta_m}^2\,\omega_2'')}\right] \quad (29)$$

Average BER expression mentioned in Eq. 29 attains the finite value if and only if the condition $\sigma_{\zeta_m}^2\,\omega_1'' \le 1$ and $\sigma_{\zeta_m}^2\,\omega_2'' \le 1$ satisfies. The accuracy of the obtained average BER expression depend on the accurate selection of the reference point $\psi_o^{(1)}$ and $\psi_o^{(2)}$ which must be lies in the integrand obtained in Eq. 29 and obtained by V_{ζ_m}. Thus, necessary and sufficient condition resulted is given as

$$\psi_o^{(1)} = V_{\zeta_m} + \omega_1'(\psi_o^{(1)})\sigma_{\zeta_m}^2 \quad (30a)$$

$$\psi_o^{(2)} = V_{\zeta_m} + \omega_2'(\psi_o^{(2)})\sigma_{\zeta_m}^2 \quad (30b)$$

Equations 30a and 30b can be solved using MATLAB software in order to obtain the value of $\psi_o^{(1)}$ and $\psi_o^{(2)}$. Initially value of $\psi_o^{(1)}$ and $\psi_o^{(2)}$ is chosen to be equal to V_{ζ_m}. The closed form expression for average BER or unconditional BER for proposed hybrid PPM–BPSK–SIM FSO under weak turbulence using wavelength diversity given in Eq. 29 can be evaluated using Eqs. 30a, 30b, ω_1', ω_2', ω_1'' and ω_2''. After performing the simplification, the values of ω_1', ω_2', ω_1'' and ω_2'' for hybrid FSO system are as follows

$$\omega_1' = -\frac{v}{\Xi_N}\bar{\gamma}I_{m_o}^2 e^{2\psi_o^{(1)}} \quad (31a)$$

$$\omega_1'' = 2\omega_1' \quad (31b)$$

$$\omega_2' = -\frac{2v}{\Xi_N}\bar{\gamma}I_{m_o}^2 e^{2\psi_o^{(2)}} \quad (31c)$$

$$\omega_2'' = 2\omega_2' \quad (31d)$$

4.1.3 Time diversity

In time diversity scheme only one wavelength has been chosen for transmission. Thus, $\lambda_1 = \lambda_2 = \lambda_3, \ldots, = \lambda$, $\sigma_{\zeta_1}^2 = \sigma_{\zeta_2}^2 = \sigma_{\zeta_3}^2, \ldots, = \sigma_{\zeta}^2$ and average BER closed form expression is obtained by making precisely the assumption mentioned in the Eq. 29 is given by

$$\begin{aligned}P_e = \frac{u_0}{2}\left(\frac{\phi^{(1)}(e^{\psi_o^{(1)}})}{\sqrt{1-\sigma_\zeta^2\omega_1''}}\right)^{\Xi_N} \cdot \left(\frac{e^{V_\zeta}}{e^{\psi_o^{(1)}}}\right)^{\Xi_N\omega_1'} \\ \cdot \exp\left[\frac{\Xi_N(\omega_1'\sigma_\zeta)^2}{2} + \frac{\Xi_N\omega_1''(V_\zeta+\omega_1'\sigma_\zeta^2-\psi_o^{(1)})^2}{2(1-\sigma_\zeta^2\omega_1'')}\right] \\ + \frac{u_1}{2}\left(\frac{\phi^{(2)}(e^{\psi_o^{(2)}})}{\sqrt{1-\sigma_\zeta^2\omega_2''}}\right)^{\Xi_N} \cdot \left(\frac{e^{V_\zeta}}{e^{\psi_o^{(2)}}}\right)^{\Xi_N\omega_2'} \\ \cdot \exp\left[\frac{\Xi_N(\omega_2'\sigma_\zeta)^2}{2} + \frac{\Xi_N\omega_2''(V_\zeta+\omega_2'\sigma_\zeta^2-\psi_o^{(2)})^2}{2(1-\sigma_\zeta^2\omega_2'')}\right]\end{aligned} \tag{32}$$

4.2 BER analysis under moderate and strong AT

4.2.1 No diversity

The statistical expectation of instantaneous conditional BER given generously by Eq. 3 with respect to the statistical GG fading random variable ζ conveys the appropriate expression of unconditional BER as

$$P_e = \int_0^\infty Q\left(\sqrt{\bar{\gamma} I_o^2 \zeta^2}\right) \frac{2(\alpha\beta)^{\frac{\alpha+\beta}{2}}}{\Gamma(\alpha)\Gamma(\beta)} \zeta^{\frac{\alpha+\beta-2}{2}} K_{\alpha-\beta}\left(2\sqrt{\alpha\beta\zeta}\right) d\zeta \tag{33}$$

By substituting the value of Q function from Eq. 3, expressing e^{-x^2} in terms of Meijer's G function as $G_{0,1}^{1,0}(x^2 \big|_0^-)$ and using the property mentioned in (Prudnikov et al. 2003)

$$\begin{aligned}\int_0^\infty x^{\tilde{\alpha}-1} K_v(bx) G_{p,q}^{m,n}\left(\omega x^{\frac{2l}{k}} \middle| \begin{matrix}(a_p)\\(b_q)\end{matrix}\right) dx \\ = \frac{\pi k^\mu (2l)^{\tilde{\alpha}-1}}{(2\pi)^{c^*(k-1)+l}(b)^{\tilde{\alpha}}} G_{kp+2l,kq}^{km,kn+2l}\left(\frac{\omega^k (2l)^{2l}}{b^{2l} k^{k(q-p)}} \middle| \begin{matrix}\Delta\left(l, 1-\frac{\tilde{\alpha}+v}{2}\right), \Delta\left(l, 1-\frac{\tilde{\alpha}-v}{2}\right), \Delta(k,(a_p))\\ \Delta(k,(b_q))\end{matrix}\right)\end{aligned} \tag{34}$$

in Eq. 33, the closed form expression of average BER can be expressed as

$$\begin{aligned}P_e = \frac{(2)^{\alpha+\beta}}{(4\pi)\Gamma(\alpha)\Gamma(\beta)}\left[\frac{u_0}{2} G_{4,1}^{1,4}\left(\frac{v\bar{\gamma} I_o^2}{2(\alpha\beta)^2} \middle| \begin{matrix}\frac{1-\alpha}{2}, \frac{2-\alpha}{2}, \frac{1-\beta}{2}, \frac{2-\beta}{2}\\ 0\end{matrix}\right)\right] \\ + \frac{(2)^{\alpha+\beta}}{(4\pi)\Gamma(\alpha)\Gamma(\beta)}\left[\frac{u_1}{2} G_{4,1}^{1,4}\left(\frac{v\bar{\gamma} I_o^2}{(\alpha\beta)^2} \middle| \begin{matrix}\frac{1-\alpha}{2}, \frac{2-\alpha}{2}, \frac{1-\beta}{2}, \frac{2-\beta}{2}\\ 0\end{matrix}\right)\right]\end{aligned} \tag{35}$$

4.2.2 Wavelength diversity

In the wavelength diversity scheme, Ξ_N different transceivers, each of them is typically transmitting the same signal at same time using appropriately different wavelengths. Each *m th* copy of received signal is accurately detected by the assigned *m th* receiver. Thus, assuming independent and identically distributed (i.i.d) bit transmission, the unconditional BER (P_e) for multiple AT channels $m = 1, 2, \dots, \Xi_N$ is given by

$$P_e = \int_0^\infty \mathrm{Q}\left(\sqrt{\frac{\bar{\gamma}}{\Xi_N}\sum_{m=1}^{\Xi_N}\left(I_{m_0}\zeta_m\right)^2}\right)\cdot\frac{2(\alpha_m\beta_m)^{\frac{\alpha_m+\beta_m}{2}}}{\Gamma(\alpha_m)\Gamma(\beta_m)}\zeta_m^{\frac{\alpha_m+\beta_m-2}{2}}K_{\alpha_m-\beta_m}\left(2\sqrt{\alpha_m\beta_m\zeta_m}\right)\mathrm{d}\zeta_m \tag{36}$$

By substituting the value of Q function from Eq. 3, expressing e^{-x^2} in terms of Meijer's G function as $G_{0,1}^{1,0}(x^2|_0^-)$ and Eq. 34 in Eq. 36, the unconditional BER can be expressed as

$$\begin{aligned} P_e = {} & \frac{u_0}{2}\prod_{m=1}^{\Xi_N}\frac{(2)^{\alpha_m+\beta_m}}{(4\pi)\Gamma(\alpha_m)\Gamma(\beta_m)}\left[G_{4,1}^{1,4}\left(\frac{\nu\bar{\gamma}I_o^2}{2\Xi_N(\alpha_m\beta_m)^2}\middle|\begin{matrix}\frac{1-\alpha_m}{2},\frac{2-\alpha_m}{2},\frac{1-\beta_m}{2},\frac{2-\beta_m}{2}\\0\end{matrix}\right)\right] \\ & +\frac{u_1}{2}\prod_{m=1}^{\Xi_N}\frac{(2)^{\alpha_m+\beta_m}}{(4\pi)\Gamma(\alpha_m)\Gamma(\beta_m)}\left[G_{4,1}^{1,4}\left(\frac{\nu\bar{\gamma}I_o^2}{\Xi_N(\alpha_m\beta_m)^2}\middle|\begin{matrix}\frac{1-\alpha_m}{2},\frac{2-\alpha_m}{2},\frac{1-\beta_m}{2},\frac{2-\beta_m}{2}\\0\end{matrix}\right)\right] \end{aligned} \tag{37}$$

4.2.3 Time diversity

Time diversity scheme employs one wavelength suitably chosen for hybrid FSO communication system. Thus, $\lambda_1 = \lambda_2 = \lambda_3, \dots, = \lambda_{\Xi_N} = \lambda$, where $\alpha_1 = \alpha_2 = \alpha_3, \dots, = \alpha_{\Xi_N} = \alpha$ and $\beta_1 = \beta_2 = \beta_3, \dots, = \beta_{\Xi_N} = \beta$. The average BER closed form expression is obtained by making the assumption in Eq. 37 is given by

$$\begin{aligned} P_e = {} & \frac{(2)^{\Xi_N\alpha+\Xi_N\beta}}{(4\pi)^{\Xi_N}(\Gamma(\alpha)\Gamma(\beta))^{\Xi_N}}\frac{u_0}{2}\left[G_{4,1}^{1,4}\left(\frac{\nu\bar{\gamma}I_o^2}{2\Xi_N(\alpha\beta)^2}\middle|\begin{matrix}\frac{1-\alpha}{2},\frac{2-\alpha}{2},\frac{1-\beta}{2},\frac{2-\beta}{2}\\0\end{matrix}\right)\right]^{\Xi_N} \\ & +\frac{(2)^{\Xi_N\alpha+\Xi_N\beta}}{(4\pi)^{\Xi_N}(\Gamma(\alpha)\Gamma(\beta))^{\Xi_N}}\frac{u_1}{2}\left[G_{4,1}^{1,4}\left(\frac{\nu\bar{\gamma}I_o^2}{\Xi_N(\alpha\beta)^2}\middle|\begin{matrix}\frac{1-\alpha}{2},\frac{2-\alpha}{2},\frac{1-\beta}{2},\frac{2-\beta}{2}\\0\end{matrix}\right)\right]^{\Xi_N} \end{aligned} \tag{38}$$

The following section discusses the implementation results using proposed closed form expression of average BER in hybrid PPM–BPSK–SIM based FSO system using no diversity, wavelength diversity and time diversity to prove the validity of the derived expressions.

5 Numerical results

The analytical and Monte Carlo simulation to efficiently compute average BER for the proposed hybrid PPM–BPSK–SIM based FSO communication system using wavelength diversity and time diversity is properly presented. The simulation has been carried out using MATLAB software to exhibit the adequacy of the proposed closed form expression over the 20*th* order Gauss Hermite approximation (GHA) in the consistent presence of lognormal and GG AT. In view to perform the valid comparisons between different order hybrid modulation schemes proposed in FSO communication system, the average transmitted data rate and optical power are kept constant. Table 1 listed system parameters and fundamental constants used appropriately in the simulation. The three different wavelengths $\lambda_1 = 850$ nm, $\lambda_2 = 1310$ nm and $\lambda_3 = 1550$ nm has been recently considered for analysis of average BER of proposed hybrid modulation based FSO communication system with diversity over weak AT (i.e. lognormal channel) and moderate and strong AT (i.e. GG channel). The other parameter considered in efficient computation is the optical transmission link distance L_d whose range varies from 500 meters to 5,000 meters.

Figure 3 shows the computed Average BER versus average SNR with progressively increasing the modulation order from 2-PPM–BPSK–SIM to 8-PPM-BPSK–SIM employed in FSO communication system in the weak AT channel conditions, using proposed closed form expression [derived in Eq. 21], GHA method and Monte Carlo simulation over 1 million iterations. It is critically observed that average BER of 10^{-9} is achieved precisely at SNR = 24 dB in specific case of 2-PPM–BPSK–SIM. 4-PPM–BPSK–SIM merely acquires same average BER at SNR of 27.5 dB and the higher modulation order achieves same average BER at higher SNR comparatively. With the increasing the numerical value of modulation order in hybrid modulation scheme, it is clearly marked that the desired value of average BER is achieved at higher SNR value comparatively which is similar in nature as presented in the literature by Faridzadeh et al. (2012), Liu et al. (2015) and Giri and Patnaik (2018). Average BER accurately computed using the proposed closed form expression obtained in Eq. 21, is consistent with Monte Carlo simulation and the used GHA method. A excellent consistency among the numerical results obtained by the proposed closed form expression and theoretical analysis clearly validates the proposed closed form expression of average BER of PPM–BPSK–SIM based FSO system.

Table 1 List of parameters

Name	Symbol	Value
Bit rate	R_b	2 Gbps
Responsivity	R	1
Optical receiver load resistance	R_L	1 kΩ
Optical receiver gain	G_r	10
Modulation index	μ_o	1
Electron charge	q	1.6×10^{-19} C
Boltzmann's constant	K_b	1.38×10^{-23} W/K/Hz
Ambient receiver noise temperature	T	300 K
Ionization factor	K_a	0.7
Angle of divergence	ϕ_r	10^{-3} radian
Amplifier noise figure	F_n	2
Receiver's aperture diameter	D	0.04 m
Link distance	L_d	1 km
Wavelength	λ	850 nm, 1310 nm, 1550 nm
Atmospheric extinction coefficient	η	0.1 dB/km

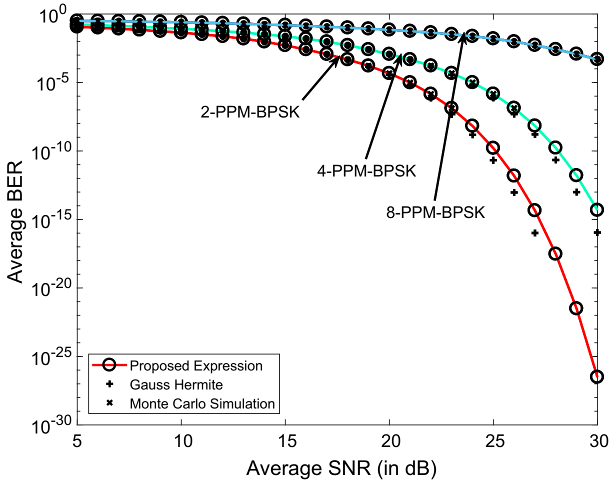

Fig. 3 Average BER versus the average SNR for varying order of hybrid PPM–BPSK–SIM based FSO communication system in the weak AT channel

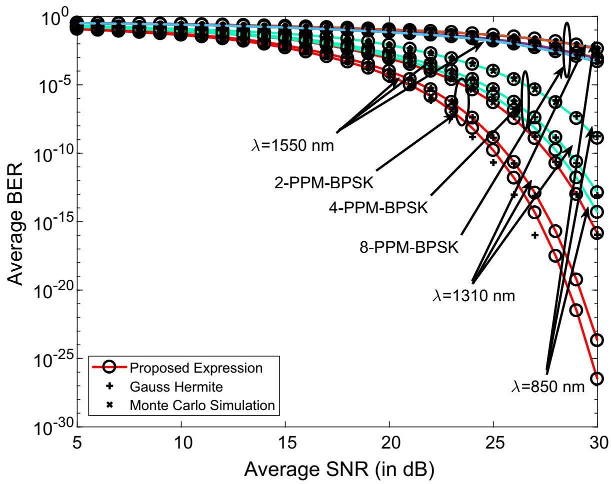

Fig. 4 Average BER versus the average SNR for 2-, 4- and 8-PPM–BPSK–SIM FSO at wavelength of 850 nm, 1310 nm, and 1550 nm in the weak AT channel

Figure 4 shows the average BER versus the average SNR for 2-PPM–BPSK–SIM, 4-PPM–BPSK–SIM and 8-PPM–BPSK–SIM at three different wavelengths, 850 nm, 1310 nm, and 1550 nm knowingly employs in FSO communication system in the weak AT channel. The possible effect of progressively increasing wavelengths is clearly depicted that average BER starts decreasing with the increase of the wavelength and decrease of modulation order. Average BER of 10^{-9} is typically achieved at 24 dB at $\lambda = 1550$ nm, 27.5 dB at $\lambda = 1310$ nm with 2-PPM–BPSK–SIM based FSO communication system.

The potential effect of observed variation in the symbol length K of the hybrid PPM–BPSK–SIM employed in implemented FSO system on its average BER performance is shown precisely in the Fig. 5. Here, the atmospheric turbulence is typically fixed at $C_n^2 = 9.866 \times 10^{-15}\ \mathrm{m}^{-2/3}$ and typically varies the symbol length in powers of 2 between 2 to 8. With the gradual increase in the size of the PPM–BPSK–SIM symbol length, average BER curve shifted towards upward right as clearly observed in the Fig. 5 and shown the consistency with the theoretical analysis. Moreover, numerical results of average BER

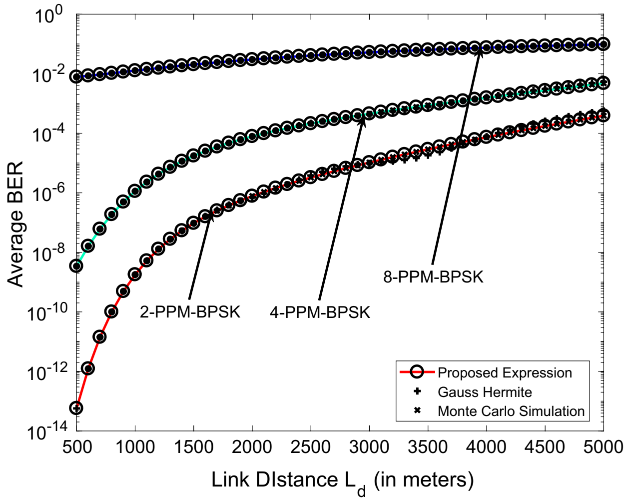

Fig. 5 Average BER versus link distance for 2-, 4- and 8-PPM–BPSK–SIM FSO at the wavelength of 1550 nm in the weak AT channel

computed using proposed closed form expression, GHA and Monte Carlo simulation shows considerable agreement with each other in this notable case also, which again confirms the validity of numerical results obtained using proposed closed form expression of average BER of hybrid PPM–BPSK–SIM based FSO system with no diversity.

It is clearly remarked from Eq. 3 that the Rytov variance depends on the wavelength and link distance used. With the gradual increase in the link distance keeping wavelength constant, Rytov variance increases. Thus, average BER versus link distance performance with varying average length of the symbol of hybrid PPM–BPSK–SIM FSO communication system is carried out at three different wavelengths used in weak AT channel and is shown in the Fig. 6. It is clearly depicted from the resulted graph that with the considerable decrease in the link distance and choosing higher wavelength, average BER appreciably

Fig. 6 Average BER versus link distance for 2-, 4- and 8-PPM–BPSK–SIM FSO at wavelength of 850 nm, 1310 nm and 1550 nm in the weak AT channel

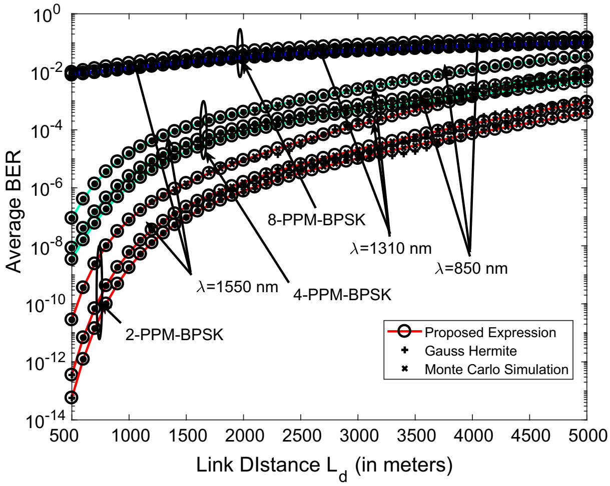

reduces and hence system performance progressively improves. In Fig. 6, it is clearly verified that numerical average BER results of proposed closed form expression, GHA and Monte Carlo simulation are consistent.

The considerable variation in average BER performance versus link distance L_d with the change in the average length of the symbol of the FSO system uses PPM–BPSK–SIM modulation is also carried out and is shown in the Fig. 6. The nature of the curves resulted is exactly matched with the theoretical analysis. Moreover, in the possible scenario of varying the length of the symbol used in hybrid system, Moreover, the proposed closed form expression for hybrid PPM–BPSK–SIM FSO communication system is not only analytically usable but also preserves the accuracy.

Simulation work assumes $\Xi_N = 3$ transceiver pair is properly used in the specific case of wavelength diversity. Figure 7 shows the possible effect of average SNR on the computed average BER of proposed system in weak AT with varying size of symbol length. The average BER of 10^{-9} can be reasonably achieved at SNR of 22.7 dB typically using 2-PPM–BPSK–SIM based FSO communication system. In this manner, FSO system performance is meaningfully improved by properly using the wavelength diversity scheme. Increase in the considerable length of gradual increase in symbol causes decrease in average BER performance. In wavelength diversity scheme, same bit of information be typically transmitted number of times and hence, the efficiency of the linkage and performance of proposed FSO communication systems can be enhanced by using diversity technique.

Figure 8 shows average BER outcome in weak AT channel against average SNR for wavelength diversity and is properly compared with the non-diversity based FSO communication system. The wavelength diversity parameter Ξ_N be typically varied from 2 to 3. It is clearly depicted that with the observed increase of Ξ_N the average BER gradually decreases. The analytical results obtained from derived expression mentioned in Eq. 29 is perfectly matched with the consistent results obtained from MC simulation and GHA.

Figure 9 shows variation in average BER with respect to the average FSO communication method SNR based on hybrid modulation scheme using diversity of wavelengths and is contrasted with the specific case with no diversity. Three different modulation order 2-, 4- and 8-PPM–BPSK–SIM scheme studied for two different wavelength diversity parameter $\Xi_N = 2$ and $\Xi_N = 3$. With the gradual increase in the Ξ_N, the average BER performance

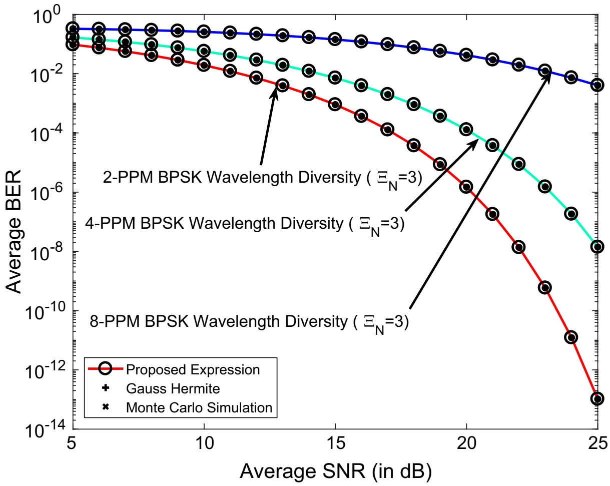

Fig. 7 Average BER performance for 2-, 4- and 8-PPM–BPSK–SIM FSO system using wavelength diversity (varying Ξ_N) in the weak AT channel

Fig. 8 Performance comparison of 4-PPM–BPSK–SIM employed FSO with and without wavelength diversity in the weak AT channel

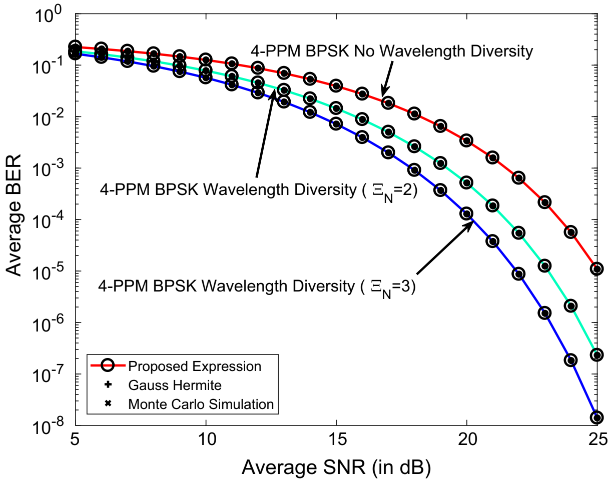

Fig. 9 Average BER performance for 2-, 4- and 8-PPM–BPSK–SIM based FSO using wavelength diversity in the weak AT channel

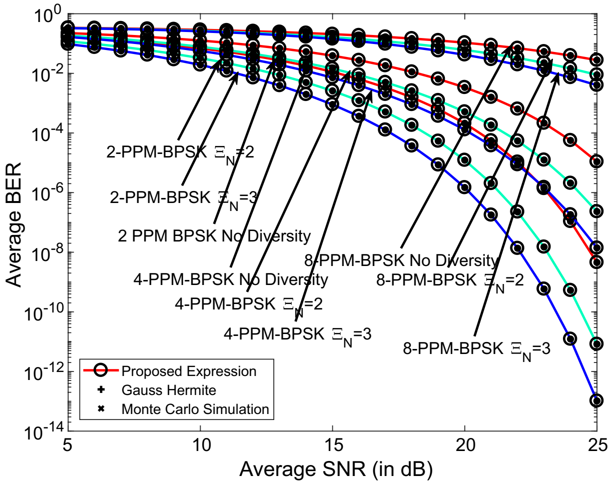

progressively improves in each possible case of symbol length of hybrid modulation scheme. Average BER performance improves effectively in each case of hybrid modulation scheme with the higher value of Ξ_N in direct comparison to no diversity case.

As in wavelength diversity, composite transmitter typically transmits the necessary information using number of distinct wavelengths towards the intended receivers simultaneously. Every intended FSO receiver accurately detects the desired signal of the information at a given wavelength. In the communication channel, the quality of signal transmission varies in respect to the signal wavelength. And, eventually, the remarkable efficiency of the average BER can be undoubtedly enhanced on the intended receiver using hybrid modulation using wavelength diversity based FSO communication system in weak AT.

Figure 10 presents the change in average BER against the average SNR for 4-PPM–BPSK–SIM using time diversity in weak AT channel condition obtained in Eq. 32. With time diversity, it is clearly demonstrated that the practical efficiency of average BER can be increased in weak AT relative to the non-diversity situation. The time diversity

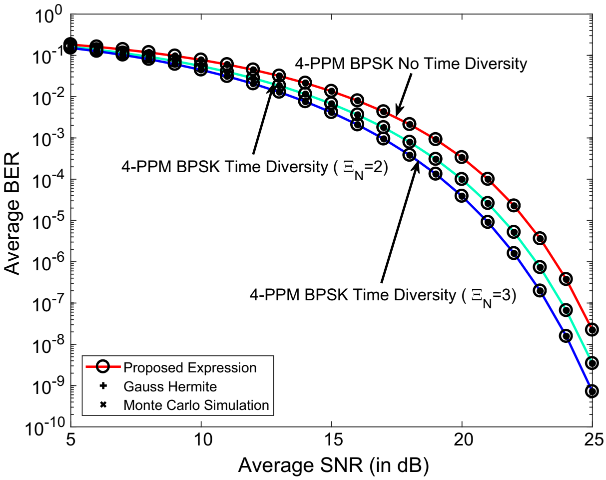

Fig. 10 Average BER curve for 4-PPM–BPSK–SIM FSO with and without time diversity in the weak AT channel

hybrid modulation based FSO communication system typically comprises of a possible pair of transmitters and receivers. But the local transmitter typically transmits the desired signal to the intended receiver over the turbulent atmospheric channel more than once in various time slots. Therefore the total effective average bit rate of the direct linkage is typically decreasing and thus increasing average BER performance. The average BER of 10^{-5} is properly obtained at SNR of 20 dB in 4-PPM–BPSK–SIM based FSO communication system using time diversity with three numbers of transceiver pairs. With the gradual decrease of considerable number of transceiver pairs and no time diversity, the performance of average BER progressively reduces.

Figure 11 accurately depicts the considerable variation of average BER with the change of average SNR for 2-PPM–BPSK–SIM, 4-PPM–BPSK–SIM and 8-PPM–BPSK–SIM based FSO communication system using time diversity with two and three numbers of receivers in the weak AT channel. It is clearly observed from Fig. 11 that the average BER performance nature against average SNR in varying time diversity parameter Ξ_N from 2 to

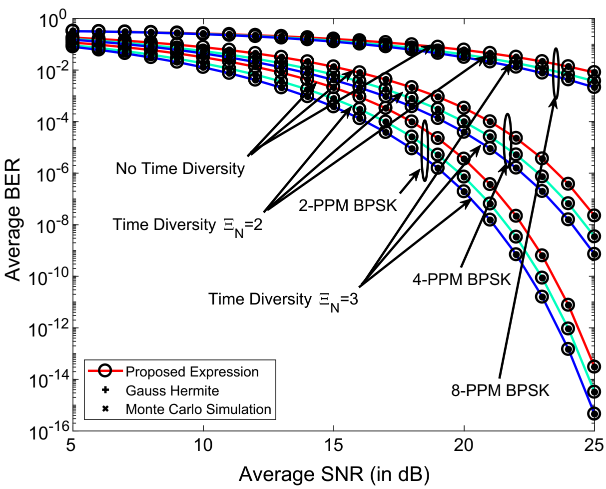

Fig. 11 Average BER against average SNR for 2-, 4- and 8-PPM–BPSK–SIM based FSO communication system with and without time diversity in the weak AT channel

3. Figure 11 also compare average BER with no diversity case for carefully evaluating the notable performance of proposed FSO in 2-PPM–BPSK–SIM, 4-PPM–BPSK–SIM and 8-PPM–BPSK–SIM, with the increase in diversity parameter which shows improvement in the average BER performance. For $\Xi_N = 3$, an hybrid modulation based FSO system gives lowest average BER of less than 10^{-6} for the practical value of average SNR above 20 dB compared to the other cases.

In Fig. 12, Eq. 35 are carefully plotted for average BER with respect to average SNR for three different hybrid modulation schemes i.e. 2-PPM–BPSK–SIM, 4-PPM–BPSK–SIM, 8-PPM–BPSK–SIM based FSO communication system in the presence of moderate and strong AT channel with no diversity at fixed $\lambda = 1550$ nm. The average BER performance become poor in moderate and poorest in strong AT channel condition. The average BER of 10^{-3} or less is obtained at average SNR of 35 dB. Average BER curves shifted upwards with the increasing the symbol length.

The possible effect of varying the selection of wavelength $\lambda_1 = 850$ nm, $\lambda_1 = 1310$ nm and $\lambda_1 = 1550$ nm in Eq. 35 under moderate and strong turbulence for three different 2-PPM–BPSK–SIM, 4-PPM–BPSK–SIM and 8-PPM–BPSK–SIM based FSO communication system is illustrated in Fig. 13. It is depicted from the Fig. 13 that the lower wavelength shows poor average BER for all three hybrid modulation scheme in comparison to the higher wavelength. Moreover, 2-PPM–BPSK–SIM based FSO system has better average BER performance in proper comparison to the 4-PPM–BPSK–SIM and 8-PPM–BPSK–SIM based FSO system typically using no diversity scheme.

In Eq. 37, varying the Ξ_N from 2 to 3 effect on the average BER as a function of average SNR for 4-PPM–BPSK–SIM based FSO communication system using wavelength diversity in comparison to no diversity in moderate and strong AT channel condition is plotted in Fig. 14. From the results, it is inferred that with the increase of diversity parameter Ξ_N causes gradually decrease in the average BER. For $\Xi_N = 3$, 4-PPM–BPSK–SIM based FSO system gives the minimum average BER of less than 10^{-4} with an average SNR value more than 35 dB comparatively.

In order to present the fair comparison for the average BER versus the average SNR in using 2-PPM–BPSK–SIM, 4-PPM–BPSK–SIM and 8-PPM–BPSK–SIM based FSO communication system using wavelength diversity and no diversity scheme at moderate and

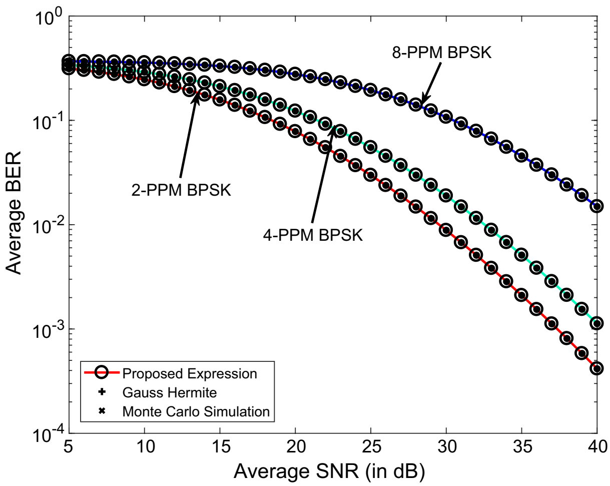

Fig. 12 Average BER curve for varying order of hybrid PPM–BPSK–SIM based FSO communication system in the moderate and strong AT channel

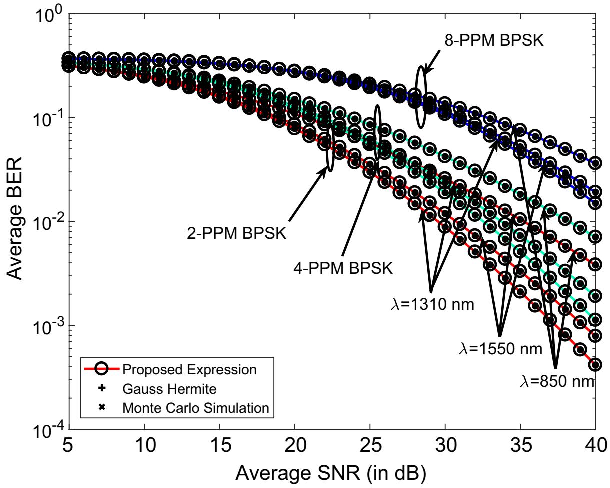

Fig. 13 Error performance for 2-, 4- and 8-PPM–BPSK–SIM FSO at wavelength of 850 nm, 1310 nm, and 1550 nm in the moderate and strong AT channel

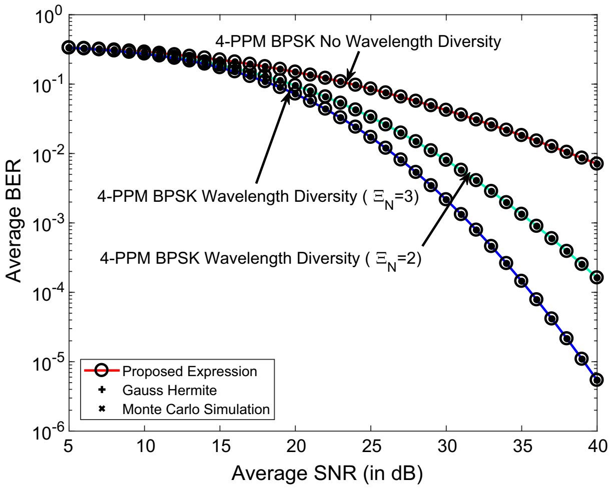

Fig. 14 Average BER comparison for 4-PPM–BPSK–SIM based FSO system with and without wavelength diversity in the moderate and strong AT channel

strong AT link is illustrated in the Fig. 15. The efficacy of AT link with lower average BER is resulted by using diversity parameter $\Xi_N = 3$ in each hybrid modulation based FSO communication.

If the diversity parameter Ξ_N is fixed and keep equal to 3 in Eq. 37 for three different 2-PPM–BPSK–SIM, 4-PPM–BPSK–SIM and 8-PPM–BPSK–SIM based FSO communication system under moderate and strong AT channel condition with wavelength diversity, then average BER is plotted in Fig. 16 as a function of average SNR. It is clearly seen the observation that with the increase of hybrid modulation symbol size, there is a gradual decrease in the average BER performance.

In Fig. 17 using the expression derived in Eq. 38, the average BER versus the average SNR for 4-PPM–BPSK–SIM based FSO communication system with increasing time diversity parameter Ξ_N from 2 to 3 in moderate and strong AT condition is plotted. The Average BER less than 10^{-5} is obtained at average SNR above than the 37 dB in the case of 4-PPM–BPSK–SIM based FSO system with diversity parameter $\Xi_N = 3$.

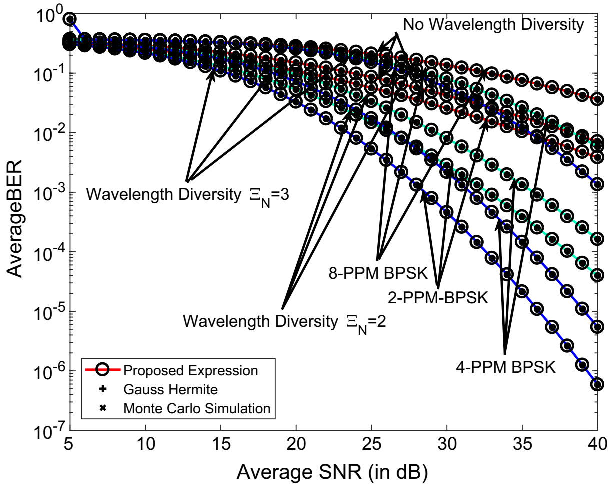

Fig. 15 Average BER performance for 2-, 4- and 8-PPM–BPSK–SIM based FSO with and without wavelength diversity in the moderate and strong AT channel

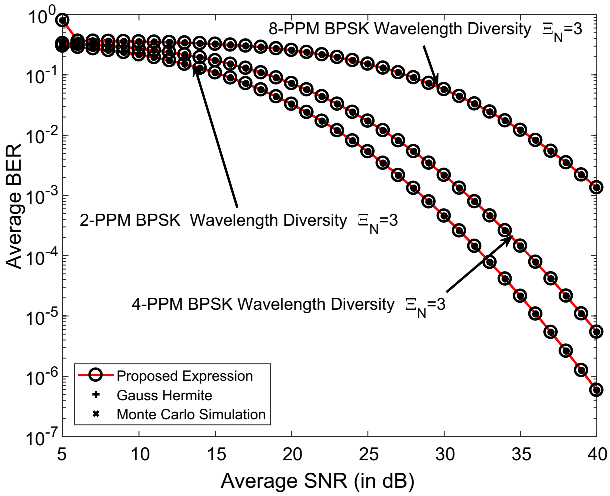

Fig. 16 Performance comparison of 2-, 4- and 8-PPM–BPSK–SIM FSO communication system using fixed wavelength diversity parameter in the moderate and strong AT channel

The increase of time diversity parameter Ξ_N from 2 to 3 in Eq. 38 impact on average BER versus the average SNR for 2-PPM–BPSK–SIM, 4-PPM–BPSK–SIM and 8-PPM–BPSK–SIM based FSO communication system is shown in the Fig. 18. The average BER performance is enhanced by using time diversity and it is further improved by increasing the time diversity parameter Ξ_N in each case of hybrid modulation employed FSO system. In both time diversity and wavelength diversity, compared with the situation without diversity, the overall average BER is considerably increased.

GHA is a numerical integration technique and its results converges to the accurate value if the range over which its approximation value is computed is chosen to be large. Moreover, GHA additionally involves the determination of corresponding weights and zeros, which makes it computationally intensive. However, the derived closed form expression is a simple to evaluate Average BER of PPM–BPSK–SIM based FSO system with both wavelength diversity, time diversity and with no diversity under all AT, shows excellent agreement in

Fig. 17 Average BER curve comparison for 4-PPM–BPSK–SIM FSO with different time diversity parameter in the moderate and strong AT channel

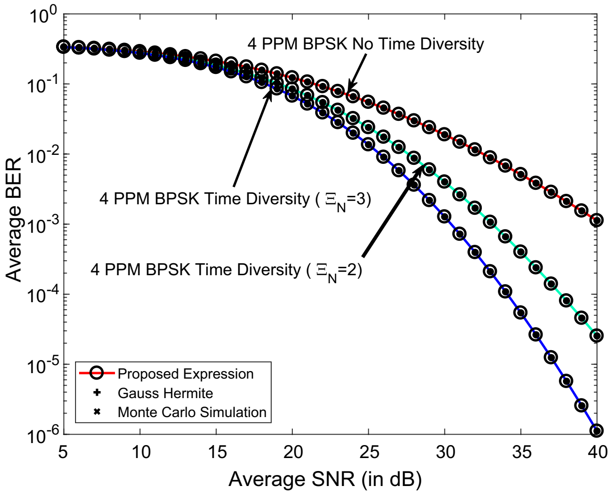

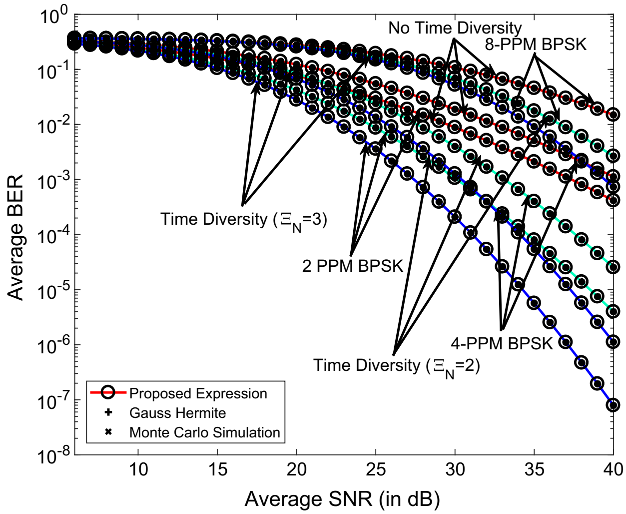

Fig. 18 Average BER comparison for 2-, 4- and 8-PPM–BPSK–SIM based FSO using time diversity with its varying parameter value from 1 to 3 in the moderate and strong AT channel

the result obtained theoretically. Moreover, the proposed closed form expression for hybrid PPM–BPSK–SIM FSO communication system derived in no diversity, wavelength diversity and time diversity in weak, moderate and strong AT channel condition, is not only analytically usable but also preserves the accuracy.

6 Conclusion

The paper has properly investigated the potential impact of lognormal and GG fading on average BER performance of FSO system under different diversity schemes for hybrid modulation scheme. Both time diversity and wavelength diversity are used to presents a novel closed form expression of average BER of hybrid modulation scheme for proposed system in convenient terms of Meijer's G function and simple elementary functions. Monte Carlo simulations unanimously confirmed that obtained results can accurately predict the performance of proposed FSO system. The consistent result adequately demonstrated the possible use of both wavelength and time diversity shows 3–7 dB average SNR improvement in proposed hybrid modulation scheme based FSO system at fixed BER = 10^{-2} in strong AT. Moreover, the effect of various parameters like the symbol length and link distance on average BER under different AT are compared, the results shows that with the gradual increase of average symbol length and link distance, the average error performance degraded gradually but have better performance with diversity comparatively. These above findings reasonably infers the hybrid PPM–BPSK–SIM with the wavelength and time diversity as a favourable system for FSO communication system, despite increased cost and considerable complexity. The hybrid scheme along with diversity properly presented in this paper will be helpful to system designers and leading researchers for 5G communication system.

References

Abaza, M.R., Mesleh, R., Mansour, A., Aggoune, E.H.M.: Diversity techniques for a free-space optical communication system in correlated log-normal channels. Opt. Eng. **53**(1), 016102 (2014)

Balaji, K., Prabu, K.: Performance evaluation of FSO system using wavelength and time diversity over malaga turbulence channel with pointing errors. Opt. Commun. **410**, 643–651 (2018)

Chatzidiamantis, N.D., Karagiannidis, G.K.: On the distribution of the sum of gamma-gamma variates and applications in RF and optical wireless communications. IEEE Trans. Commun. **59**(5), 1298–1308 (2011)

Chiani, M., Dardari, D., Simon, M.K.: New exponential bounds and approximations for the computation of error probability in fading channels. IEEE Trans. Wireless Commun. **2**(4), 840–845 (2003)

Ding, J., Yu, S., Fu, Y., Ma, J., Tan, L.: New approximate and asymptotic closed-form expressions for the outage probability and the average BER of MIMO-FSO system with MRC diversity technique over Gamma-Gamma fading channels with generalized pointing errors. Opt. Commun. **456**, 124633 (2020)

Faridzadeh, M., Gholami, A., Ghassemlooy, Z., Rajbhandari, S.: Hybrid pulse position modulation and binary phase shift keying subcarrier intensity modulation for free space optics in a weak and saturated turbulence channel. JOSA A **29**(8), 1680–1685 (2012)

Feng, F., White, I.H., Wilkinson, T.D.: Aberration correction for free space optical communications using rectangular zernike modal wavefront sensing. J. Lightwave Technol. **32**(6), 1239–1245 (2014)

Gappmair, W., Flohberger, M.: Error performance of coded FSO links in turbulent atmosphere modeled by gamma-gamma distributions. IEEE Trans. Wirel. Commun. **8**(5), 2209–2213 (2009)

Ghassemlooy, Z., Popoola, W., Rajbhandari, S.: Optical Wireless Communications: System and Channel Modelling with Matlab®. CRC Press, Boca Raton (2012)

Giri, R.K., Patnaik, B.: BER analysis and capacity evaluation of FSO system using hybrid subcarrier intensity modulation with receiver spatial diversity over log-normal and gamma-gamma channel model. Opt. Quant. Electron. **50**(6), 231 (2018)

Héliot, F., Ghavami, M., Nakhai, M.R.: An accurate closed-form approximation of the average probability of error over a log-normal fading channel. IEEE Trans. Wirel. Commun. **7**(5), 1495–1500 (2008)

Islam, M.S., Majumder, S.: Analytical evaluation of the cross-polarization induced crosstalk on BER performance of an OFDM FSO link with polarization diversity. Opt. Commun. **474**, 126095 (2020)

Ji, J., Wu, B., Zhang, J., Xu, M., Wang, K.: Enhancement of reliability and security in a time-diversity FSO/CDMA wiretap channel. OSA Continuum **2**(5), 1524–1538 (2019)
Ji, J., Wu, B., Zhang, J., Xu, M., Wang, K.: Design and Investigation of 10 Gb/s FSO wiretap channel using OCDMA time-diversity reception. IEEE Photonics J. **2**(3), 1–12 (2020)
Kaushik, R., Khandelwal, V., Jain, R.: A new closed form approximation for BER for optical wireless systems in weak atmospheric turbulence. J. Opt. Commun. **39**(2), 247–253 (2018)
Khandelwal, V., et al.: A new approximation for average symbol error probability over log-normal channels. IEEE Wirel. Commun. Lett. **3**(1), 58–61 (2014)
Khichar, S., Inaniya, P.K.: Evaluation of performance of Is-OWC OFDM system with spatial diversity. In: Janyani, V., Singh, G., Tiwari, M., Ismail, T. (eds.) Optical and Wireless Technologies, pp. 49–55. Springer, Berlin (2020)
Li, J., Liu, J.Q., Taylor, D.P.: Optical communication using subcarrier PSK intensity modulation through atmospheric turbulence channels. IEEE Trans. Commun. **55**(8), 1598–1606 (2007)
Liu, H., Liao, R., Wei, Z., Hou, Z., Qiao, Y.: BER analysis of a hybrid modulation scheme based on PPM and MSK subcarrier intensity modulation. IEEE Photonics J. **7**(4), 1–10 (2015)
Majumdar, A.K.: Advanced Free Space Optics (FSO): A Systems Approach, vol. 186. Springer, Berlin (2014)
Navidpour, S.M., Uysal, M., Kavehrad, M.: BER performance of free space optical transmission with spatial diversity. IEEE Trans. Wirel. Commun. **6**(8), 2813–2819 (2007)
Nistazakis, H.E.: A time-diversity scheme for wireless optical links over exponentially modeled turbulence channels. Optik **124**(13), 1386–1391 (2013)
Nouri, H., Uysal, M.: Experimental investigation on the effect of wavelength on aperture averaging in FSO communications. Opt. Lett. **45**(11), 3063–3066 (2020)
Olabiyi, O., Annamalai, A.: Invertible exponential-type approximations for the Gaussian probability integral Q(x) with applications. IEEE Wirel. Commun. Lett. **1**(5), 544–547 (2012)
Popoola, W.O., Ghassemlooy, Z.: BPSK subcarrier intensity modulated free-space optical communications in atmospheric turbulence. J. Lightwave Technol. **27**(8), 967–973 (2009)
Prabu, K., Cheepalli, S., Kumar, D.S.: Analysis of PolSK based FSO system using wavelength and time diversity over strong atmospheric turbulence with pointing errors. Opt. Commun. **324**, 318–323 (2014)
Prudnikov, A.P., Bryčkov, J.A., Maričev, O.I.: Integrals and Series. More special functions, vol. 3. Gordon and Breach, London (2003)
Shah, D., Kothari, D.: Performance analysis of free space optical link with wavelength diversity under weak and moderate turbulence conditions. Sens. Lett. **17**(2), 137–143 (2019)
Shankar, P.M.: Fading and Shadowing in Wireless Systems. Springer, Berlin (2017)
Sharma, K., Grewal, S.K.: Capacity analysis of free space optical communication system under atmospheric turbulence. Opt. Quant. Electron. **52**(2), 82 (2020)
Srivastava, V., Mandloi, A., Soni, G.G.: Outage probability and average BER estimation of FSO system employing wavelength diversity. Opt. Quant. Electron. **51**(7), 229 (2019)
Trisno, S., Davis, C.C.: Performance of free space optical communication systems using polarization shift keying modulation. In: Free-Space Laser Communications VI, vol. 6304, p. 63040V (2006)
Tsiftsis, T.A., Sandalidis, H.G., Karagiannidis, G.K., Uysal, M.: Optical wireless links with spatial diversity over strong atmospheric turbulence channels. IEEE Trans. Wirel. Commun. **8**(2), 951–957 (2009)
Uysal, M., Li, J., Yu, M.: Error rate performance analysis of coded free space optical links over gamma-gamma atmospheric turbulence channels. IEEE Trans. Wirel. Commun. **5**(6), 1229–1233 (2006)
Varotsos, G.K., Nistazakis, H.E., Gappmair, W., Sandalidis, H.G., Tombras, G.S.: SIMO subcarrier PSK FSO links with phase noise and non-zero boresight pointing errors over turbulence channels. IET Commun. **13**(7), 831–836 (2019)
Viswanath, A., Jain, V.K., Kar, S.: Aperture averaging and receiver diversity for fso downlink in presence of atmospheric turbulence and weather conditions for OOK, M-PPM and M-DPPM schemes. Opt. Quant. Electron. **48**(9), 435 (2016)
Wainright, E., Refai, H.H., Sluss Jr., J.J.: Wavelength diversity in free-space optics to alleviate fog effects. In: Free-Space Laser Communication Technologies XVII, vol. 5712, pp. 110–118 (2005)
Wilck, M.: A general approximation method for solving integrals containing a lognormal weighting function. J. Aerosol Sci. **32**(9), 1111–1116 (2001)
Xarcha, V., Stassinakis, A., Nistazakis, H., Latsas, G., Hanias, M., Tombras, G., Tsigopoulos, A.: Wavelength diversity/or free space optical systems: performance evaluation over log normal turbulence channels. In: 2012 19th International Conference on Microwaves, Radar & Wireless Communications, vol. 2, pp. 678–683 (2012)
Yang, Y.: Performance of free-space optical communication systems using circle polarization shift keying with spatial diversity receivers. Chin. Opt. Lett. **11**, S20101 (2013)

Zhang, R., Peng, P.C., Li, X., Liu, S., Zhou, Q., He, J., Chen, Y.W., Shen, S., Yao, S., Chang, G.K.: 4x100-Gb/s PAM-4 FSO transmission based on polarization modulation and direct detection. IEEE Photonics Technol. Lett. **31**(10), 755–758 (2019)
Zhu, X., Kahn, J.M.: Free-space optical communication through atmospheric turbulence channels. IEEE Trans. Commun. **50**(8), 1293–1300 (2002)